



UNIVERSITY OF LEEDS

This is a repository copy of *Thermal energy storage enhancement of a binary molten salt via in-situ produced nanoparticles*.

White Rose Research Online URL for this paper:
<http://eprints.whiterose.ac.uk/105958/>

Version: Accepted Version

Article:

Luo, Y, Du, X, Awad, A et al. (1 more author) (2017) Thermal energy storage enhancement of a binary molten salt via in-situ produced nanoparticles. *International Journal of Heat and Mass Transfer*, 104. pp. 658-664. ISSN 0017-9310

<https://doi.org/10.1016/j.ijheatmasstransfer.2016.09.004>

© 2016. This manuscript version is made available under the CC-BY-NC-ND 4.0 license
<http://creativecommons.org/licenses/by-nc-nd/4.0/>

Reuse

Unless indicated otherwise, fulltext items are protected by copyright with all rights reserved. The copyright exception in section 29 of the Copyright, Designs and Patents Act 1988 allows the making of a single copy solely for the purpose of non-commercial research or private study within the limits of fair dealing. The publisher or other rights-holder may allow further reproduction and re-use of this version - refer to the White Rose Research Online record for this item. Where records identify the publisher as the copyright holder, users can verify any specific terms of use on the publisher's website.

Takedown

If you consider content in White Rose Research Online to be in breach of UK law, please notify us by emailing eprints@whiterose.ac.uk including the URL of the record and the reason for the withdrawal request.



eprints@whiterose.ac.uk
<https://eprints.whiterose.ac.uk/>

Thermal energy storage enhancement of a binary molten salt via in-situ produced nanoparticles

Yan Luo^{1,3}, Xiaoze Du^{1†}, Afrah Awad³, Dongsheng Wen^{2,3†}

1 School of Energy, Power and Mechanical Engineering, North China Electric Power University, Beijing 102206, China.

2 School of Aeronautic Science and Engineering, Beihang University, Beijing 100191, PR China

3 School of Chemical and Process Engineering, University of Leeds, Leeds, UK

Abstract

Thermal energy storage (TES) system is an essential component of any concentrating solar thermal power (CSP) plant to ensure a reliable plant operation even at night or cloudy weather. To enhance the TES capacity, a one-step method was proposed to synthesize nano-salts by in-situ production of CuO nanoparticles, via a high temperature decomposition of copper oxalate, in a binary salt used as a phase change material (PCM). The specific heat of the nano-salt both for solid and liquid phases were measured by differential scanning calorimetry (DSC) with the weight fraction of CuO nanoparticles varied from 0.1 to 3.0 wt %. The maximum specific heat increment of 7.96% in solid phase and 11.48% in liquid phase, were achieved at a CuO nanoparticle concentration of 0.5 wt %. A forming of intermediate layers composing of needle-like structures between nanoparticles and the salt was observed. The mixing model considering such an intermediate layer can be used to explain the observed specific heat enhancement at low particle

† Corresponding author. Email address: duxz@ncepu.edu.cn (X. Du); D.Wen@leeds.ac.uk (D. Wen)

concentrations. Both latent heat and onset temperature were decreased with increasing concentrations of CuO nanoparticles, while the melting temperature range was increased. When considering both latent heat and sensible heat contributions, the maximum increment of TES was achieved as 4.71% at 0.5 wt % CuO concentration in the temperature range from 160 °C to 300 °C.

Keywords: one-step synthesis method, binary salt, nano-salt, specific heat, thermal energy storage

1. Introduction

Thermal energy storage (TES) system is an essential component of any concentrating solar thermal power (CSP) plant to ensure a reliable plant operation even at night or cloudy weather [1-2]. There are typically four types of thermal energy storage materials, namely, sensible heat material, latent heat material, thermochemical material and adsorption material. For a CSP, inorganic salts have been widely used as both sensible and latent heat materials because of their low vapor pressure, low viscosity, and excellent thermal stability under high temperature.

However, few inorganic salts possess desirable values on both thermal conductivity (k) and specific heat (c_p), two most important properties of any TES material. For example, the specific heat of the commonly used solar salt is around 1.5 J/(g K) [3], which is quite low when compared with water. Introducing nanoparticle into a base fluid to improve its thermophysical properties, termed as 'nanofluid', has been extensively studied in the past [4-8]. Recently, similar concept was used to disperse suitable particles in solar salts to improve their thermal energy storage capacity [9-17], hence termed as 'nano-salt' here to consider the dispersion in both solid and liquid phases suitable for TES applications.. A majority of the work [18-24] showed that the specific heat of nano-salt was increased, except the experimental results of Lu et al. [20]. For example, Shin and Banerjee [4] dispersed silica nanoparticles into alkali metal chloride salt eutectics, and reported a c_p enhancement of 14.5% at 1 wt % particle concentration. Ho and Pan [17] showed that a maximum enhancement of specific heat of 19.9% was obtained at 0.063 wt % by dispersing Al_2O_3 nanoparticles into the Hitec eutectic. Lasfargues et al. [18] reported a c_p increase of 10.48% at 0.1 wt % by dispersing CuO nanoparticles into a binary mixture of nitrate. Such enhancements are surprising results as the specific heat of the nano-salt should be lower than the base salt, according to the mixture rule as

follows [21],

$$(c_p)_{nf} = \frac{(\phi\rho c_p)_{np} + (\phi\rho c_p)_{bm}}{(\phi\rho)_{np} + (\phi\rho)_{bm}} \quad (1)$$

in which c_p is the specific heat, ϕ is the volume fraction, and ρ is density. The subscripts of nf, np and bm refer to the nano-salt, nanoparticle and base material, respectively. As typical nanoparticles used have low c_p values, a small c_p of the nano-salt would be expected.

To explain the deviation of the experimental results from the traditional prediction, Shin and Banerjee [4] proposed three thermal transport mechanisms, including (1) higher c_p of nanoparticles than the bulk material, (2) higher interfacial thermal resistance due to large solid-fluid interface areas, and (3) layering of liquid molecules at the surface to form semi-solid layers. Clearly the mechanism 1) is not a plausible explanation as most c_p of nanoparticles are still lower than the base salt even after considering a c_p enhancement over their bulk counterparts. To verify the second mechanism, Andreu-Cabedo et al. [6] calculated solid-fluid interfacial area based on scanning electron microscope (SEM) images and dynamic light scattering (DLS) data, and concluded that there was an optimal nanoparticle concentration corresponding to the maximum interfacial area in the range of specific heat enhancement. According to the SEM images, Ho and Pan [17] obtained that increasing interfacial area may be the reason for the enhancement of specific heat and a slight agglomeration of nanoparticles was better for c_p improvement. Based on the third mechanism, Shin and Banerjee [9] took the semi-solid layer into consideration and modified Eq. (1) as follows,

$$(c_p)_{ns} = \frac{(\phi\rho c_p)_{np} + (\phi\rho c_p)_l + (\phi\rho c_p)_f}{(\phi\rho)_{np} + (\phi\rho)_l + (\phi\rho)_f} \quad (2)$$

where subscripts of l and f refer to the semi-solid layer and bulk base fluid, respectively. The specific heat of the semi-solid layer was assumed larger than the bulk base salt, so the specific heat

of nano-salt was enhanced. On the basis of Eq. (2), Hentschke et al. [22] built an interacting mesolayer model to explain why there was an optimal nanoparticle concentration for specific heat enhancement. The model assumed that the influence of nanoparticles on the surrounding liquid is of a long range nature, and there may have overlaps between interfacial layers of nanoparticles, which varied with different nanoparticle concentrations. So in terms of specific heat enhancement, the optimal nanoparticle concentration depended on the extent of interfacial area overlapping. However it is still quite debatable on the exact reasons for c_p enhancement.

Among all the work published, nano-salt preparation was based on the two-step method [4]. In this method, nanoparticles were produced first, and then mixed with the salt. The mixture was dissolved in water, which was sonicated and fully evaporated to form nano-salts. For the two-step synthesis method, nanoparticles need to be prepared and stored in advance, which inevitably includes many agglomerations. Considering the close relationship between the structures and properties, the disperse status of nanoparticles in the salts will play a crucial role in determining the c_p value of the nano-salt. Consequently the preparation method for nano-salt becomes significantly important, which may also be responsible for the inconsistency reported.

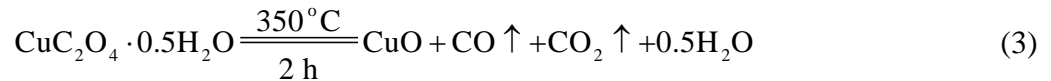
In addition, most of the research was focused on nano-salt as a sensible heat storage material. A few studies showed that the enhancement of the specific heat in liquid phase was larger than that in the solid phase [9-12]. Recently, Chieruzzi [16, 19] proposed to use a TES capacity of nano-salt, including that of both sensible and latent heat, as an evaluation criterion for phase change material (PCM) based TES materials. This study will develop a new way of forming nano-salt as PCM for TES, and determine the c_p value in a wide temperature range suitable for both sensible and latent heat storage. In addition, the optimal nanoparticle concentration and the mechanism of specific heat

enhancement will be discussed.

2. Experimental procedure

2.1 One step formation of nano-salts

Sodium nitrate (FISHER, Loughborough, UK) with 98% purity, potassium nitrate (SIGA-ALDRICH, Suffolk, UK) with 98% purity and copper oxalate hemihydrate (ALFA AESAR, Lancashire, UK) with 98% purity were purchased. Before the mixing of salts, sodium nitrate and potassium nitrate were heated separately in a furnace at 300 °C for 30 min to eliminate any humidity and impurities. Binary salt with 60 wt % NaNO₃ and 40 wt % KNO₃ was used as a base material since it was used widely in TES systems in CSP plants [23]. The reaction formula of high temperature decomposition of copper oxalate was as follows,



This temperature of 350°C and heating duration of 2 hours were based on many attempts to produce proper CuO particles for the reaction. Similar parameters were also suggested by Hong [24], who reported that CuO nanoparticles could be produced directly by high temperature decomposition. So this chemical reaction could occur at the same time when the binary salt was melted. Sodium nitrate, potassium nitrate and copper oxalate hemihydrate were grinded and mixed at a certain ratio by a grinder for 20 minutes. Then the mixture was heated in a muffle furnace for 2 hours at the temperature of 350 °C. Finally the product containing nanoparticles was grinded again into fine powder for 60 minutes. The synthesis procedure of the nano-salt is shown in Fig. 1.

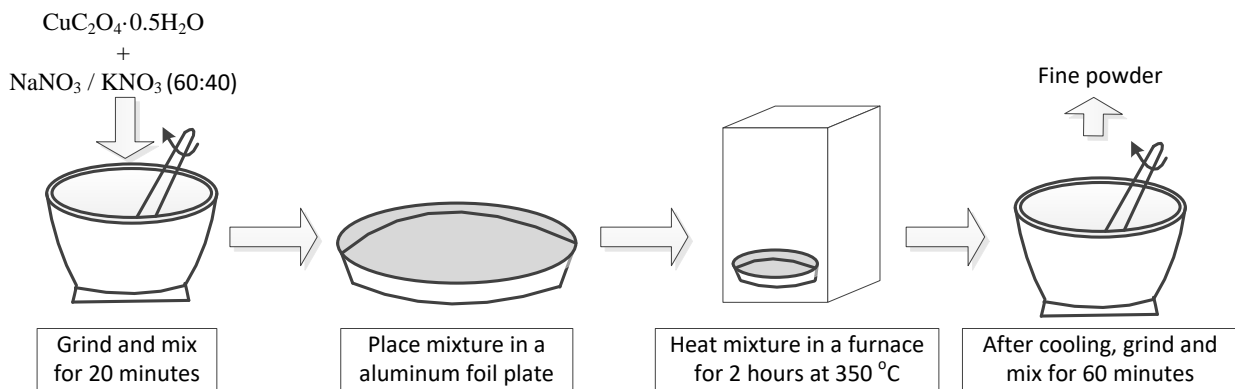


Fig. 1. One-step formation of nano-salts.

Pure binary salt, pure CuO nanoparticle and five one-step formed nano-salts with different CuO nanoparticle concentrations of 0.1 wt %, 0.5 wt %, 1.0 wt %, 2.0 wt %, 3.0 wt % were prepared independently for the experiments.

2.2 Nanoparticle characterization

X-ray Diffraction (XRD, Bruker D8) test was performed to verify that after the high temperature decomposition, the only product was copper oxide nanocrystal. Material characteristic analyses were performed by a scanning electron microscopy (SEM, FEI Nova NanoSEMTM) and a Transmission Electron Microscopy (TEM, FEI Tecnai TF20).

Differential scanning Calorimetry (DSC) was used to characterize the thermal properties for formed materials including specific heat, latent heat and onset melting temperature. DSC tests were performed on a DSC (DSC1, Mettler Toledo) for pure binary salt, pure CuO nanoparticle and nano-salt with CuO concentrations of 0.1 wt %, 0.5 wt %, 1.0 wt %, 2.0 wt %, 3.0 wt % respectively. For each nanoparticle concentration, three samples were prepared. The specific heat measurements were carried out through a standard procedure using a sapphire reference pan. Briefly,

empty standard Tzero aluminum lids/pans (TA Instruments, Inc) were weighed on a balance first, and then 30 grams of samples were added into the pans with hermetic lids. To remove any adsorbed moisture, the samples were heated and dried in the DSC at 300 °C for 30 min before the thermal cycle, and the final weight was obtained after each experiment.

The thermal cycle included an isothermal heating of 10 minutes at 160 °C, a constant rate heating at 2 °C/min from 160 °C to 300 °C, an isothermal heating of 5 minutes at 300 °C, and then cooling from 300 °C to 160 °C at 40 °C/min. The heating rate of 2 °C/min was similar to xx and xx, in order to achieve a more uniform temperature distribution within the sample with improved instrument's resolution. Each sample was consecutively tested for three times, leading to totally 9 tests for one particle concentration. The specific heat of sapphire was first tested in order to identify the validity of the experiment. Compared with the literature value, the experimental error was within $\pm 1\%$.

3. Results and discussions

Fig. 2 shows the XRD spectrum of copper oxalate decomposition product. The position of the diffraction peak is well consistent with that of the standard JCPDS of copper oxide with monoclinic structure. No characteristic peaks of impurities or other precursor compounds were observed. Based on the Scherrer equation,

$$D_c = K\lambda / (\beta \cos\theta) \quad (4)$$

the XRD spectrum gives that the diameter of copper oxide crystal is about 14 nm. Fig.3 gives the TEM image of copper oxalate decomposition product after the DSC experiments. Agglomeration of CuO nanoparticle was observed. The average particle size was about 20 nm, which was not far from the value estimated from XRD data. Therefore, both methods suggest that synthesized particle is in

the range of 10~20 nm.

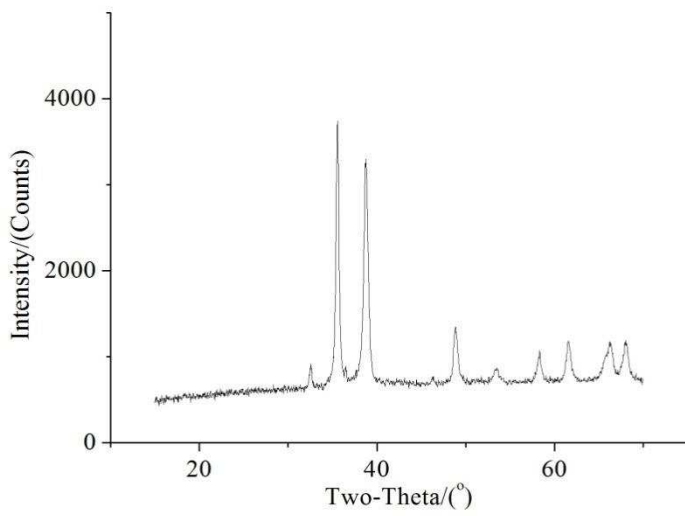


Fig. 2. The XRD spectrum of copper oxalate decomposition product.

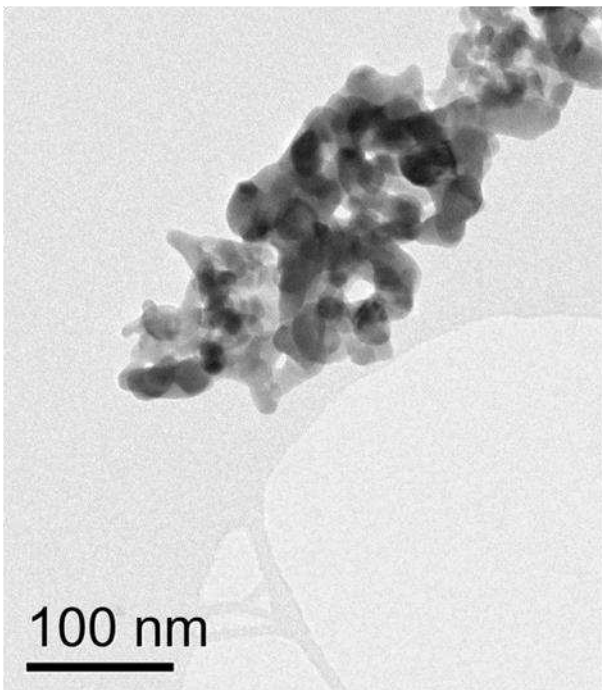
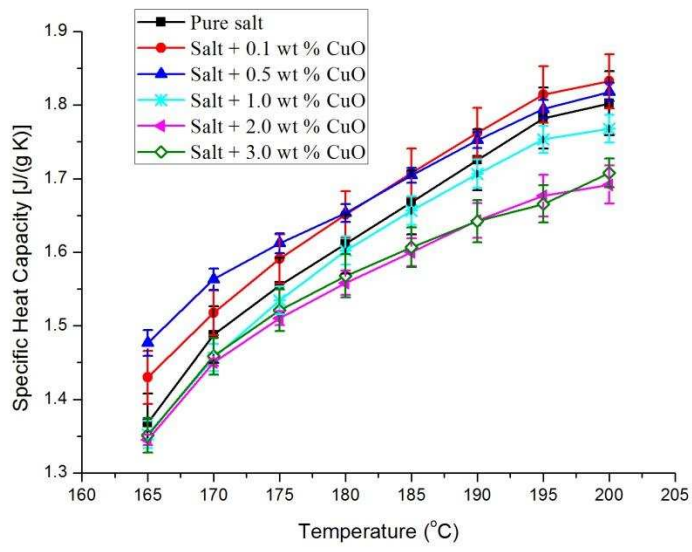


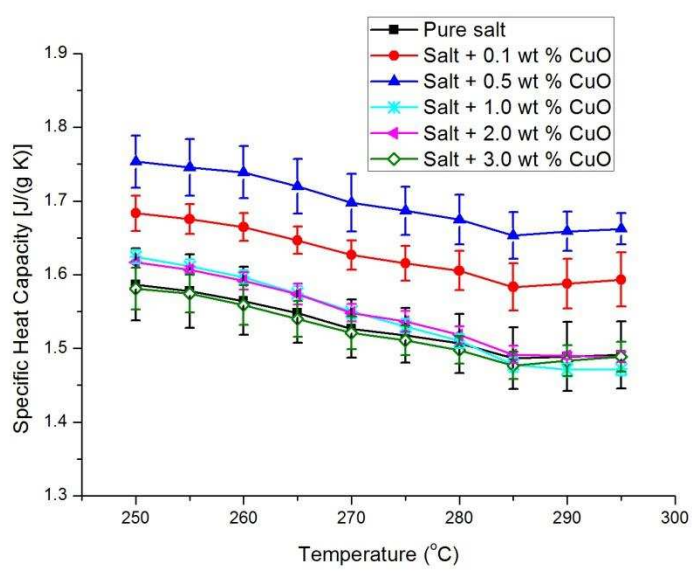
Fig. 3. The TEM image of copper oxalate decomposition product.

Fig. 4(a) and (b) show the variations of the specific heat of the pure salt and five nano-salts with

temperature in solid and liquid phases. For the solid phase, it could be seen that the specific heat of different CuO concentrations increased with increasing temperature. For the liquid phase, the specific heat first decreased with increasing temperature, and then approached to constant values as the temperature was higher than 285 °C.



(a) Solid phase.



(b) Liquid phase.

Fig. 4. Variation of the specific heat of pure binary salt and nano-salts with temperature.

Table 1. Percentage increase in specific heat compared to pure salt for different concentrations of CuO nanoparticle.

Temperature	Pure salt	0.1 wt % CuO	0.5 wt % CuO	1.0 wt % CuO	2.0 wt % CuO	3.0 wt % CuO
$^{\circ}\text{C}$	Specific heat J/(g K)	Increase %	Increase %	Increase %	Increase %	Increase %
165 (solid)	1.37	4.55	7.96	-1.14	-1.67	-1.22
250 (liquid)	1.58	6.09	10.5	2.38	1.89	-0.35
270 (liquid)	1.52	6.55	11.21	1.53	1.42	-0.36
295 (liquid)	1.49	6.86	11.48	-1.27	-0.19	-0.15

The quantitative results of the specific heat increment by nano-salts under different concentrations of CuO nanoparticles compared with that of the pure binary salt were listed in Table 1. The maximum enhancement of the specific heat was obtained by nano-salt at a concentration of 0.5 wt % CuO. For the solid phase, the maximum enhancement was 7.96% at the temperature of 165 $^{\circ}\text{C}$. For the liquid phase, the maximum enhancement was 11.48% at the temperature of 295 $^{\circ}\text{C}$. The specific heat of nano-salt with 0.1 wt % CuO and 0.5 wt % CuO increased at certain degree for both solid and liquid phases. However, it showed little enhancement or even decrease of the specific heat of the nano-salts while the concentration of CuO nanoparticle became equal or higher than 1.0 wt %.

The present results are different from that of Lasfargues et al. [18], of which the optimum ratio of CuO nanoparticles was 0.1 wt %. The deviation may mainly due to different sizes and different production processes of CuO nanoparticles.

Table 2 gives latent heat, onset temperature, melting temperature and total storage capacity of pure salt and nano-salts with different concentrations of CuO nanoparticles. It can be obtained that the latent heat was decreased from 107.99 kJ/kg to 96.56 kJ/kg when increasing the percentage of CuO nanoparticles from 0.0 wt % to 3.0 wt %. However, Chieruzzi et al. [16] pointed out that the latent heat of 1.0 wt % $\text{SiO}_2+\text{Al}_2\text{O}_3$ was 17.23 kJ/kg higher than that of the pure salt. Experimental results of Lasfargues et al. [18] also showed that the latent heat of nano-salt with 0.1 wt % CuO was increased by 2.4 kJ/kg compared with that of the pure salt. It was speculated that the increment was due to the formation of nano-structures near the solid wall of the particles. It is difficult to compare the results directly due to different synthesis methods used. The structures formed via our one-step method may have salient difference to others reported. In addition, it is also possible the formation of nano-structures may not be the only reason of the modification of latent heat. Binary salt and nano-salts are not pure materials, and they would have a melting temperature range instead of an exact melting temperature. The melting range is defined as the span of temperature from the onset temperature at which the sample first begin to liquefy to the temperature where the entire sample is melt. When increasing the concentration of CuO nanoparticles from 0.0 wt % to 3.0 wt %, the onset temperature was decreased from 220.47 °C to 212.22 °C and the melting temperature was increased from 229.45 °C to 236.35 °C. Therefore, the melting temperature range was also increased with the increase of particle concentration.

By considering both latent heat and sensible heat, the total thermal energy storage (TES) capacity

was calculated as follows,

$$\text{Total_TES_capacity} = \frac{\int_{160^{\circ}\text{C}}^{300^{\circ}\text{C}} h(T)dT}{m dT / dt} \quad (5)$$

in which, h is heat flow, T is working temperature, m is the weight of the sample, dT/dt is heating rate. Similar to the results listed in Table 1, the total TES capacity of 1.0 wt %, 2.0 wt % and 3.0 wt % CuO nanoparticles were lower than that of the pure salt, while the TES capacity for the nano-salt with 0.1 wt % CuO nanoparticles was increased by 9.65 kJ/kg. The maximum increase was also identified at 0.5 wt %, i.e 15.53 kJ/kg. It appears that for the given temperature range, the sensible heat had greater influence on the total TES capacity than that of the latent heat under lower nanoparticle concentrations. Fig. 5 shows the trend of TES capacity versus temperature for pure binary salt and nano-salts. It is clear to see that the optimal concentration was 0.5 wt % CuO when using nano-salt as PCM in the temperature range from 160 °C to 300 °C.

Table 2. Results of the latent heat, onset temperature, melting temperature and total thermal energy storage capacity (160°C ~ 300°C).

Material	Latent heat kJ/kg	Onset temperature °C	Melting temperature °C	Total TES capacity kJ/kg
Pure salt	107.99	220.47	229.45	329.79
Salt + 0.1 wt % CuO	106.04	217.82	230.14	339.44
Salt + 0.5 wt % CuO	103.38	215.78	232.68	345.32
Salt + 1.0 wt % CuO	102.54	214.75	233.86	328.43
Salt + 2.0 wt % CuO	99.11	213.71	235.71	323.47

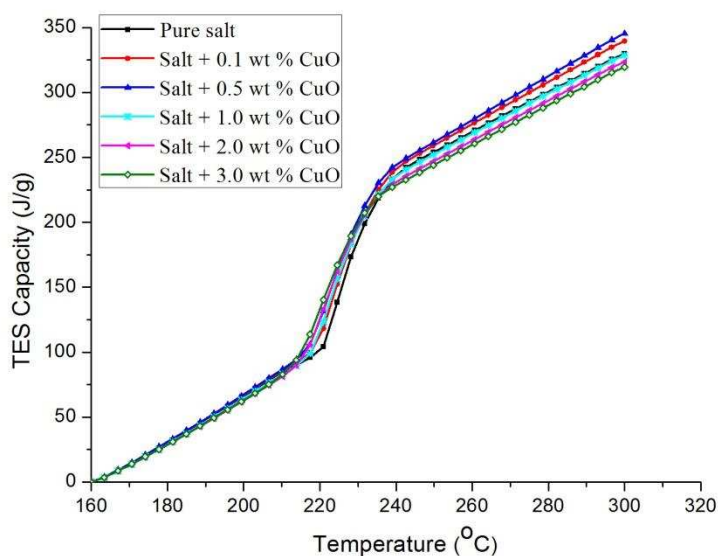


Fig. 5. Variation of the TES capacity of pure binary salt and nano-salts with temperature.

To examine the effect of CuO only, pure CuO nanoparticle was produced directly by heating copper oxalate for 2 hours at the temperature of 350 °C, and the specific heat was measured by the same method by the DSC. Fig. 6 shows the variation of the specific heat of CuO nanoparticles with temperature. The average value of the specific heat is 0.67 J/(g K) in the temperature range from 165 °C to 295 °C. Zhou et al. [25] referred that the specific heat of bulk CuO was 0.54 J/(g K). Thus the specific heat of CuO nanoparticle was enhanced by up to 24% compared with that of the bulk CuO. This result is consistent with both theoretical and experimental observations that the specific heat increases with the decrease of particle size especially at the nanometer scale. For example, Wang et al. [26] experimentally observed that the specific heat of Al₂O₃ nanoparticle was 25% higher than the bulk value, and a large specific surface area was thought to be responsible [27].

Although the specific heat of nanoparticle is higher than the bulk value, it is still lower than that of the present pure binary salt. If based on Eq. (1), the specific heat of nano-salt should be lower than that of the pure salt, which was the cases for high CuO concentrations (i.e. ≥ 1 w%), as indicated in Table 1. However it clearly cannot explain the case of low particle concentrations, further enhancement mechanism, instead of conventional macroscale heat transfer, is discussed below.

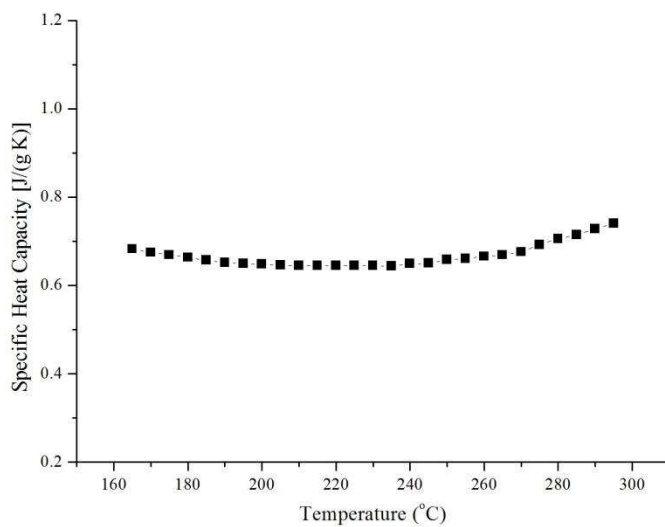


Fig. 6. Specific heat of CuO nanoparticles.

In order to reveal the enhancement mechanism of nano-salts, SEM images that illustrated the micro structure were acquired for the pure binary salt, as well as for the nano-salts with different concentrations of CuO nanoparticle, which were displayed in Fig. 7. Fig. 7(a) shows the general pure binary salt structures, while Fig. 7(b) to (f) show the images of the microstructures of the nano-salts with various concentrations of CuO nanoparticle.

According to the SEM images, isolated nanoparticles were not easy to be detected. Measurements of solid-fluid interfacial area had to be based on high-size clusters. So it could not be

accurate to obtain the relationship between solid-fluid interfacial area and specific heat enhancement and verify the mechanism 2) mentioned in section 1.

Compared with the pure binary salt shown in Fig. 7(a), some special needle-like nano-structures were formed for the nano-salts in Fig. 7(b) and (c), of which the concentrations of CuO nanoparticle was 0.1 wt % and 0.5 wt %, respectively. However, almost no needle-like nano-structure was discovered at higher concentrations, as shown in Fig. 7(d)-(f). Among all the concentrations, 0.5 wt % CuO nanoparticle shown in Fig. 7(c) had the most needle-like structures, which is coincident with the maximum increase in the specific heat. It seems that more needle-like nano-structures would lead to high specific heat increase and so controlled forming of such structures is important in further increasing the value of specific heat.

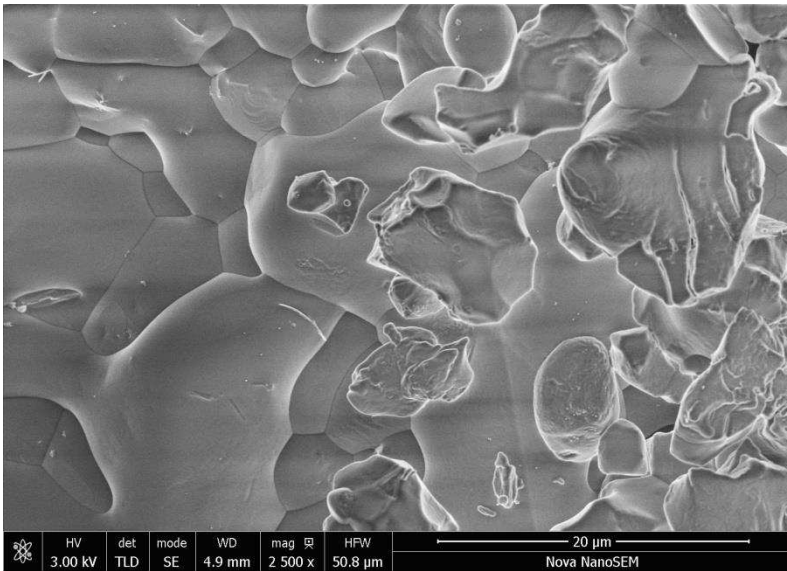
Similarly, Tiznobaik et al. [15] proposed that the specific heat enhancement was due to the formation of needle-like nano-structures, which was a semi-solid layer on the surface of the nanoparticles and was formed by the molten salt molecules. These needle-like nano-structures had very large specific surface areas and could lead to large surface energy and higher specific heat than that of the pure salt, resulting in a c_p enhancement. Shin and Banerjee [9] also observed similar nano-structures and specific heat enhancement. They referred that transformed phase of salts were nucleated by nanoparticles and grown to form nano-structures. The specific heat of the semi-solid layer was assumed to be 6.0 J/(g K) , which corresponded to the property value at the melting point of the salt. By applying this assumption and Eq. (2), their predictions were in good agreement with their experimental data.

Based on experimental results and Eq. (2), the specific heat and mass fraction of the semi-solid layer for both liquid and solid phases are further illustrated here. For nano-salt at the liquid phase,

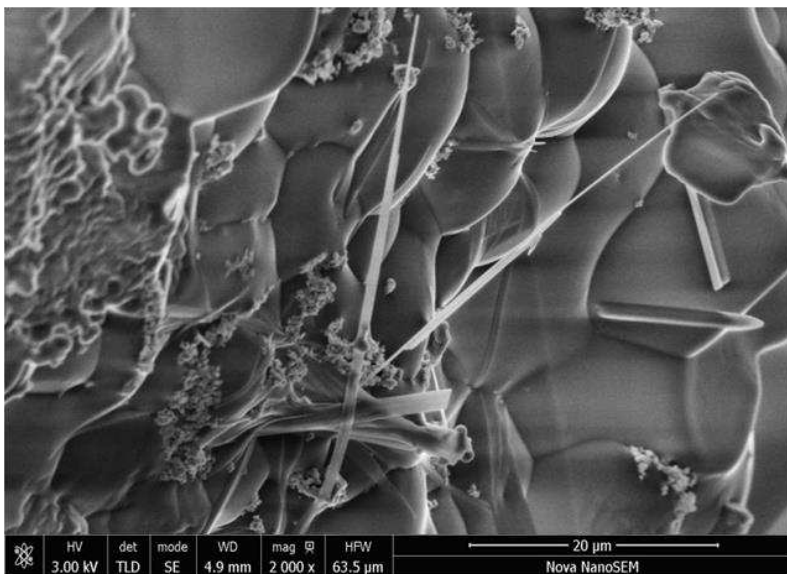
the specific heat of the semi-solid layer is assumed to be 9.0 J/(g K) , which is the property value at the melting point of the base salt. According to the measurement results, the specific heat of nanoparticle, pure salt and nano-salt with 0.5 wt \% CuO nanoparticle were respectively 0.74 J/(g K) , 1.49 J/(g K) and 1.66 J/(g K) at the temperature of $295 \text{ }^\circ\text{C}$. Based on Eq. (2), the mass fraction of semi-solid layer was obtained as 2.31 wt \% for nano-salt with 0.5 wt \% CuO nanoparticle. Similarly, the mass fraction of the 0.1 wt \% of CuO was calculated as 1.34 wt \% . Considering that the mass fraction of semi-solid layer should be the same for both liquid and solid phases, the possible c_p value of this semi-solid layer at the solid phase of nano-salt could be determined in a similar way. Based on the experimental specific heat data, i.e., 0.68 J/(g K) , 1.37 J/(g K) and 1.48 J/(g K) respectively at $T=165 \text{ }^\circ\text{C}$ for nanoparticle, pure salt and 0.5 wt\% nano-salt, the specific heat of the semi-solid layer at $T=165 \text{ }^\circ\text{C}$ was calculated as 6.27 J/(g K) , which is lower than the value at the liquid phase of nano-salt. Using this value, the specific heat of nano-salt with 0.1 wt \% CuO nanoparticle at $T =165 \text{ }^\circ\text{C}$ could be predicted as 1.43 J/(g K) , which is almost the same as the measurement result. It appears that with proper assumption of specific heat of semi-solid layer, the mixing model of Eq. (2) could be used for specific heat prediction. A large mass fraction of a semi-solid layer with a higher c_p value could be used to explain the increase in the specific heat of nano-salts.

However, it is unclear why the amount of needle-like nano-structures, namely mass fraction of semi-layer, does not increase monotonically with increasing CuO nanoparticle concentrations. For low particle concentrations, i.e., $<0.5 \text{ wt \%}$, there would have insufficient nanoparticle-salt interfaces to form needle-like nano-structures. For higher concentrations, as shown in Fig. 7 (d) to (f), CuO nanoparticles tend to form agglomerations, which may again impede the formation of the

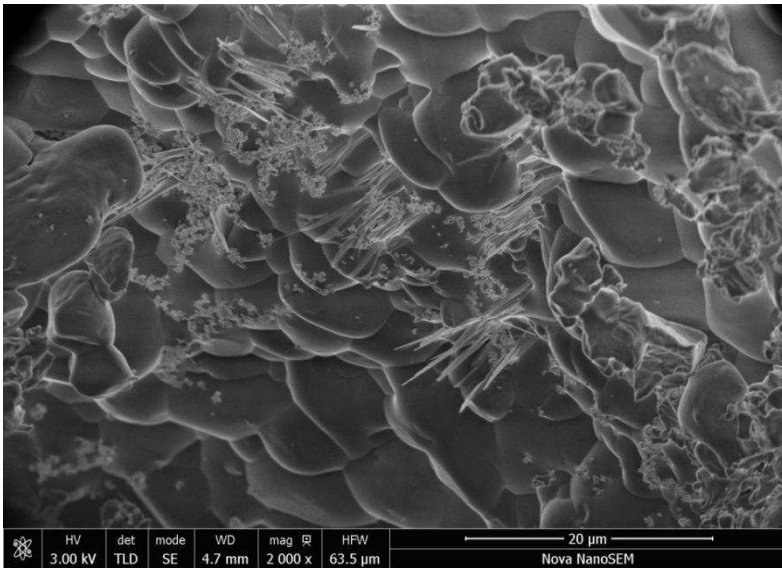
needle-like nano-structures, resulting in a decrease in interfacial area between nanoparticle and salt molecule. At this situation, the overall specific heat of the composite is more likely to follow the rule described in Eq. (1).



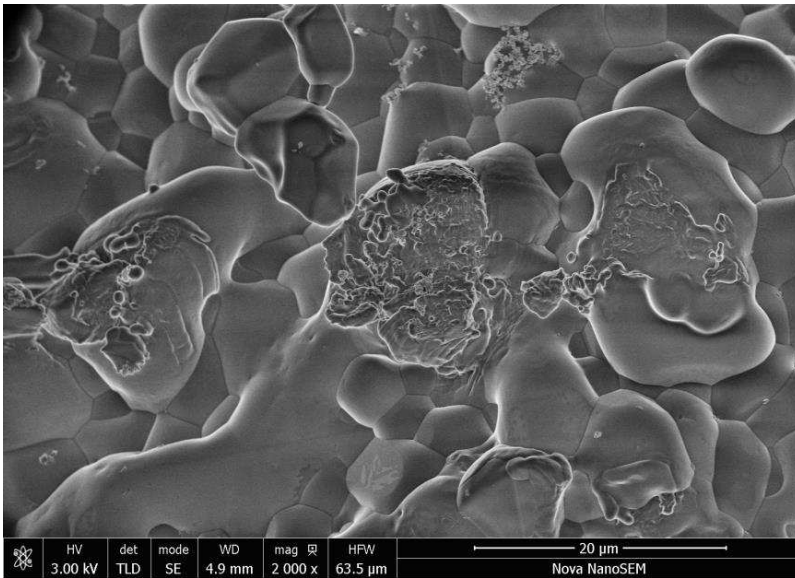
(a) Pure binary salt.



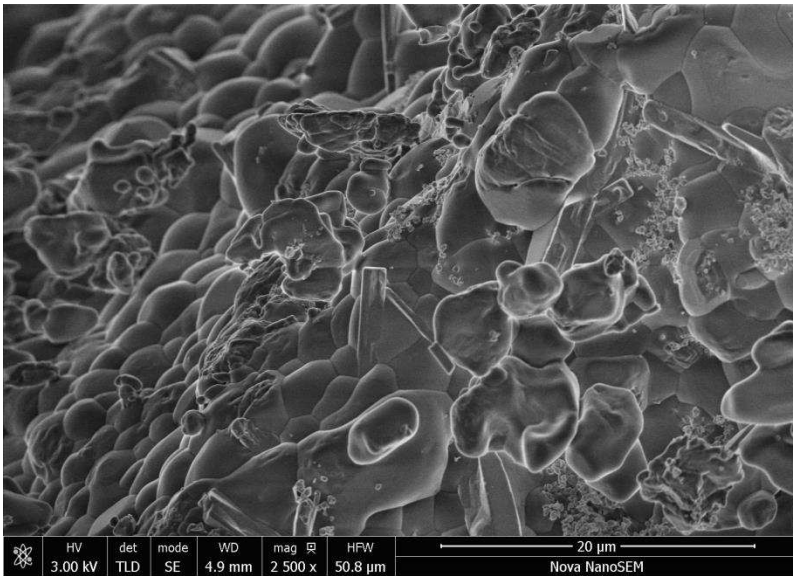
(b) Binary salt with 0.1% CuO nanoparticle.



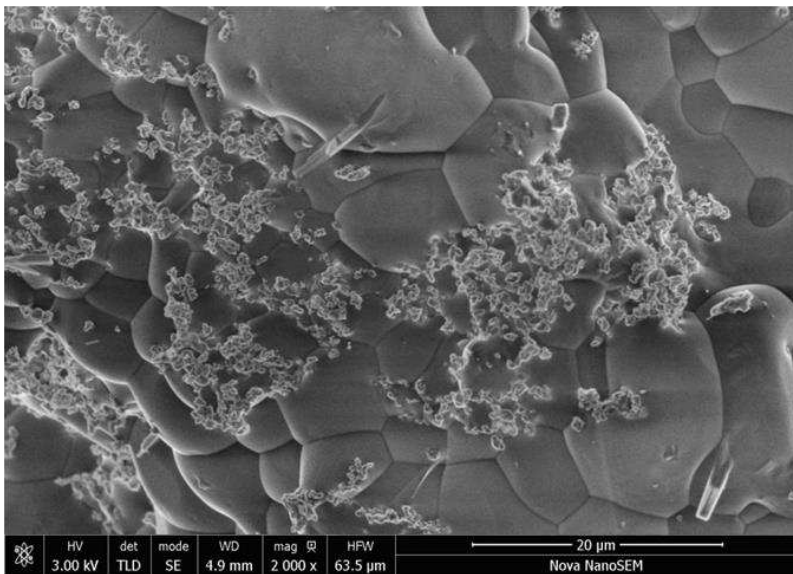
(c) Binary salt with 0.5% CuO nanoparticle.



(d) Binary salt with 1% CuO nanoparticle.



(e) Binary salt with 2% CuO nanoparticle.



(f) Binary salt with 3% CuO nanoparticle.

Fig. 7. SEM image of the micro structure of the pure binary salt and nano-salts.

4. Conclusions

A novel one-step method of synthesizing nano-salts composing of binary salt (60 wt % NaNO_3 +

40 wt % KNO_3) and different concentrations of CuO nanoparticles was validated in this work and the main results can be summarized as,

(1) DSC showed that the specific heat of different CuO concentrations increased with increasing temperature for the solid phase, while a reverse trend was found for the liquid phase. The maximum enhancement of specific heat occurred at a nanoparticle concentration of 0.5 wt %, with 7.96% increment for the solid phase and 11.48% increment for the liquid phase.

(2) The specific heat of CuO nanoparticles measured by DSC was 24% higher than that of the bulk value, which was still lower than the pure salt. So the enhancement of the specific heat of nano-salts cannot be explained by the conventional macro-scale transport mechanism.

(3) By assuming a proper mass fraction of semi-solid layer with an appropriate c_p value, the mixing model with an intermediate layer, i.e., Eq. (2), can be used to predict specific heat enhancement at low particle concentrations. The intermediate layer shall be related to the forming of needle-like structures between nanoparticles and the salt.

(4) When increasing concentrations of CuO nanoparticles, both latent heat and onset temperature were decreased, but the melting temperature range was increased. Considering both latent heat and sensible heat contributions, the maximum increment of the total storage capacity was 15.53 kJ/kg, i.e., a 4.71% enhancement over the base salt, in the temperature range from 160 °C to 300 °C at a CuO nanoparticle concentration of 0.5 wt %.

Acknowledgments

The financial supports for this research project from the National Natural Science Foundation of China (No.U1361108), the national “973 Program” of China (No. 2015CB251503), the 111 Project

(B12034) and the Fundamental Research Funds for the Central Universities (No. 2016XS30) are gratefully acknowledged.

References

- [1] Kuravi S, Trahan J, Goswami DY, Rahman MM, Stefanakos EK. Thermal energy storage technologies and systems for concentrating solar power plants. *Progress in Energy and Combustion Science* 2013; 39(4): 285-319.
- [2] Laing D, Bahl C, Bauer T, Lehmann D, Steinmann WD. Thermal energy storage for direct steam generation. *Solar Energy* 2011; 85(4): 627-633.
- [3] Tian Y, Zhao CY. A review of solar collectors and thermal energy storage in solar thermal applications. *Applied Energy* 2013; 104: 538-553.
- [4] Buongiorno J, Venerus D etc A benchmark study on the thermal conductivity of nanofluids. *Journal of Applied Physics* (2009) 106, 094312
- [5] Venerus D, Buongiorno etc. Viscosity measurement of colloidal dispersion (nanofluids) for heat transfer applications. *Applied Rheology*, 2010, 20 (4), 44582.
- [6] Wen DS, Corr M, Hu X and Lin G. Boiling heat transfer of nanofluids: The effect of heating surface modification. *International Journal of Thermal Science* 2011 50 (4), 480-485
- [7] Vafaei, S and Wen DS. Critical Heat Flux (CHF) of subcooled flow boiling of alumina nanofluids in a horizontal Microchannel. *Journal of Heat Transfer –Transactions of ASME*, 2010, 132 Article Number: 102404
- [8] Wen, DS, Influence of nanoparticles on boiling heat transfer . *Applied Thermal Engineering*, 2012, 2-9

- [9] Shin D, Banerjee D. Enhancement of specific heat capacity of high-temperature silica-nanofluids synthesized in alkali chloride salt eutectics for solar thermal-energy storage applications. *International Journal of Heat and Mass Transfer* 2011; 54(5): 1064-1070.
- [5] Schuller M, Shao Q, Lalk T. Experimental investigation of the specific heat of a nitrate–alumina nanofluid for solar thermal energy storage systems. *International Journal of Thermal Sciences* 2015; 91: 142-145.
- [6] Andreu-Cabedo P, Mondragon R, Hernandez L, Martinez-Cuenca R, Cabedo L, Julia JE. Increment of specific heat capacity of solar salt with SiO₂ nanoparticles. *Nanoscale research Letters* 2014; 9(1): 1-11.
- [7] Shin D, Banerjee D. Enhanced specific heat of silica nanofluid. *ASME Journal of Heat Transfer* 2011; 133(2): 024501.
- [8] Shin D, Banerjee D. Specific heat of nanofluids synthesized by dispersing alumina nanoparticles in alkali salt eutectic. *International Journal of Heat and Mass Transfer* 2014; 74: 210-214.
- [9] Shin D, Banerjee D. Enhanced specific heat capacity of nanomaterials synthesized by dispersing silica nanoparticles in eutectic mixtures. *ASME Journal of Heat Transfer* 2013; 135(3): 032801.
- [10] Shin D, Banerjee D. Effects of silica nanoparticles on enhancing the specific heat capacity of carbonate salt eutectic (work in progress). *The International Journal of Structural Changes in Solids* 2010; 2(2): 25-31.
- [11] Shin D, Jo B, Kwak H, Banerjee D. Investigation of high temperature nanofluids for solar thermal power conversion and storage applications. In: *Proceedings of the 14th International*

Heat Transfer Conference: 2010 Aug 8-13; Washington, DC, USA. American Society of Mechanical Engineers; 2010: 583-591.

- [12] Dudda B, Shin D. Effect of nanoparticle dispersion on specific heat capacity of a binary nitrate salt eutectic for concentrated solar power applications. *International Journal of Thermal Sciences* 2013; 69: 37-42.
- [13] Jo B, Banerjee D. Enhanced specific heat capacity of molten salt-based carbon nanotubes nanomaterials. *ASME Journal of Heat Transfer* 2015; 137(9): 091013.
- [14] Jo B, Banerjee D. Enhanced specific heat capacity of molten salt-based nanomaterials: Effects of nanoparticle dispersion and solvent material. *Acta Materialia* 2014; 75: 80-91.
- [15] Tiznobaik H, Shin D. Enhanced specific heat capacity of high-temperature molten salt-based nanofluids. *International Journal of Heat and Mass Transfer* 2013; 57(2): 542-548.
- [16] Chieruzzi M, Cerritelli GF, Miliozzi A, Kenny JM. Effect of nanoparticles on heat capacity of nanofluids based on molten salts as PCM for thermal energy storage. *Nanoscale research letters* 2013; 8(1): 1-9.
- [17] Ho MX, Pan C. Optimal concentration of alumina nanoparticles in molten Hitec salt to maximize its specific heat capacity. *International Journal of Heat and Mass Transfer* 2014; 70: 174-184.
- [18] Lasfargues M, Geng Q, Cao H, Ding Y. Mechanical dispersion of nanoparticles and its effect on the specific heat capacity of impure binary nitrate salt mixtures. *Nanomaterials* 2015; 5(3): 1136-1146.
- [19] Chieruzzi M, Miliozzi A, Crescenzi T, et al. A new phase change material based on potassium nitrate with silica and alumina nanoparticles for thermal energy storage. *Nanoscale research*

letters 2015; 10(1): 1.

- [20] Lu MC, Huang CH. Specific heat capacity of molten salt-based alumina nanofluid. *Nanoscale research letters* 2013; 8(1): 1-7.
- [21] Xuan Y, Roetzel W. Conceptions for heat transfer correlation of nanofluids. *International Journal of heat and Mass transfer* 2000; 43(19): 3701-3707.
- [22] Hentschke R. On the specific heat capacity enhancement in nanofluids. *Nanoscale research letters* 2016; 11(1): 1.
- [23] Slocum AH, Codd DS, Buongiorno J, Forsberg C, McKrell T, Nave J, Papanicolas CN, Ghobeity A, Noone CJ, Passerini S, Rojas F, Mitsos A. Concentrated solar power on demand. *Solar Energy* 2011; 85(7): 1519-1529.
- [24] Hong W. A novel preparation method to nanometer CuO powder. *Chinese Journal of Explosives and Propellants* 2000; 23(3): 7-8.
- [25] Zhou LP, Wang BX. Size and surface effects on the effective thermal conductivity of low concentration non-metallic nanoparticles. *Chinese Journal of Progress in Natural Science* 2003; 13(4): 426-429.
- [26] Wang L, Tan Z, Meng S, Liang D, Li G. Enhancement of molar heat capacity of nanostructured Al₂O₃. *Journal of Nanoparticle Research* 2001; 3(5-6): 483-487.
- [27] Wang BX, Zhou LP, Peng XF. Surface and size effects on the specific heat capacity of nanoparticles. *International Journal of Thermophysics* 2006; 27(1): 139-151.

Table captions

Table 1. Percentage increase in specific heat compared to pure salt for different concentrations of CuO nanoparticle.

Table 2. Results of the latent heat, onset temperature, melting temperature and total thermal energy storage capacity (160 °C ~ 300 °C).

Figure captions

Fig. 1. One-step formation of nano-salts.

Fig. 2. The XRD spectrum of copper oxalate decomposition product.

Fig. 3. The TEM image of copper oxalate decomposition product.

Fig. 4. Variation of the specific heat of pure binary salt and nano-salts with temperature. (a) Solid phase. (b) Liquid phase.

Fig. 5. Variation of the TES capacity of pure binary salt and nano-salts with temperature.

Fig. 6. Specific heat of CuO nanoparticles.

Fig. 7. SEM image of the micro structure of the pure binary salt and nano-salts. (a) Pure binary salt. (b) Binary salt with 0.1% CuO nanoparticle. (c) Binary salt with 0.5% CuO nanoparticle. (d) Binary salt with 1% CuO nanoparticle. (e) Binary salt with 2% CuO nanoparticle. (f) Binary salt with 3% CuO nanoparticle.